Available online at www.sciencedirect.com
ScienceDirect
Nuclear Physics B 810 (2009) 226–245
NUCLEAR PHYSICS B
www.elsevier.com/locate/nuclphysb

The flavor-changing single-top quark production in the littlest Higgs model with T parity at the LHC

Xuelei Wang *, Yanju Zhang, Huiling Jin, Yanhui Xi

College of Physics and Information Engineering, Henan Normal University, Xinxiang, Henan 453007, PR China

Received 6 October 2008; received in revised form 27 October 2008; accepted 3 November 2008

Available online 7 November 2008

Abstract

The littlest Higgs model with discrete symmetry named "T-parity" (LHT) is an interesting new physics model which does not suffer strong constraints from electroweak precision data. One of the important features of the LHT model is the existence of new source of FC interactions between the SM fermions and the mirror fermions. These FC interactions can make significant loop-level contributions to the couplings tcV, and furthermore enhance the cross sections of the FC single-top quark production processes. In this paper, we study some FC single-top quark production processes, $pp \to t\bar{c}$ and $pp \to tV$, at the LHC in the LHT model. We find that the cross sections of these processes strongly depend on the mirror quark masses. The processes $pp \to t\bar{c}$ and $pp \to tg$ have large cross sections with heavy mirror quarks. The observation of these FC processes at the LHC is certainly the clue of new physics, and further precise measurements of the cross sections can provide useful information about the free parameters in the LHT model, specially about the mirror quark masses.

PACS: 14.65.Ha; 12.60.-i; 12.15.Mn; 13.85.Lg

1. Introduction

On the experimental aspect, the forthcoming generation of high energy colliders, headed by the Large Hadron Collider (LHC) at CERN depicts an exciting scenario for probing the existence of physics beyond the Standard Model (SM) of strong and electroweak (EW) interaction [1]. For the probe of new physics at the high energy colliders like the LHC, there are two ways: one

* Corresponding author.
E-mail address: wangxuelei@sina.com (X. Wang).

0550-3213/$ – see front matter
doi:10.1016/j.nuclphysb.2008.11.002

is through detecting the direct production of new particles and the other is through unravelling the quantum effects of new physics in some sensitive and well-measured processes. These two aspects can be complementary and offer a consistent check for new physics. If the collider energy is not high enough to produce the heavy new particles, probing the quantum effects of new particles will be the only way of peeking at the hints of new physics.

On the other hand, as the heaviest fermion in the SM, the top quark is speculated to be a sensitive probe of new physics. Due to the small statistics of the experiments at the Fermilab Tevatron collider, so far the top quark properties have not been precisely measured and there remained a plenty of room for new physics effects in top quark processes. Since the LHC will be a top factory and allow to scrutinize the top quark nature, unravelling new physics effects in various top quark processes will be an intriguing channel for testing new physics models. Furthermore, there exists a typical property for the top quark in the SM, i.e., its flavor-changing (FC) interactions are extremely small [2] due to the Glashow–Iliopoulos–Maiani (GIM) mechanism. This will make the observation of any FC top quark process a smoking gun for new physics. Therefore, the combination of the top quark and FC processes will be an interesting research field for LHC experiments.

On the theoretical aspect, the SM is in excellent agreement with the results of particle physics experiments, in particular with the EW precision measurements, thus suggesting that the SM cutoff scale is at least as large as 10 TeV. Having such a relatively high cutoff, however, the SM requires an unsatisfactory fine-tuning to yield a correct ($\approx 10^2$ GeV) scale for the squared Higgs mass, whose corrections are quadratic and therefore highly sensitive to the cutoff. This little hierarchy problem has been one of the main motivations to elaborate new physics. Recently, an alternative known as the little Higgs mechanism [3], has been proposed. Such mechanism that makes the Higgs "little" in the current reincarnation of the PGB idea is collective symmetry breaking. Collective symmetry breaking protects the Higgs by several symmetries under each of which the Higgs is an exact Goldstone. Only if the symmetries are broken collectively, i.e. by more than one coupling in the theory, can the Higgs pick up a contribution to its mass and hence all one-loop quadratic divergences to the Higgs mass are avoided. The most compact implementation of the little Higgs mechanism is known as the littlest Higgs (LH) model [4]. In this model, the SM is enlarged to incorporate an approximate $SU(5)$ global symmetry. This symmetry is broken down to $SO(5)$ spontaneously, though the mechanism of this breaking is left unspecified. The Higgs is an approximate Goldstone boson of this breaking. In this model there are new vector bosons, a heavy top quark and a triplet of heavy scalars in addition to the SM particles. These new particles can make significant tree-level contributions to the experimental observables. So the original LH model suffers strong constraints from electroweak precision data [5]. The most serious constraints result from the tree-level corrections to precision electroweak observables due to the exchanges of the additional heavy gauge bosons, as well as from the small but non-vanishing vacuum expectation value (VEV) of the additional weak-triplet scalar field. To solve this problem, a Z_2 discrete symmetry named "T-parity" is introduced [6]. The littlest Higgs model with T parity (LHT), requires the introduction of "mirror fermions" for each SM fermion doublet. The mirror fermions are odd under T-parity and can be given large masses and the SM fields are T-even. T parity explicitly forbids any tree-level contribution from the heavy gauge bosons to the observables involving only Standard Model particles as external states. It also forbids the interactions that induce the triplet VEV. As a result, in the LHT model, the corrections to the precision electroweak observables are generated at loop-level. This implies that the constraints are generically weaker than those in the tree-level case, and fine tuning can be avoided [7].

As we know, there exist new sources of FC top quark interactions in some new physics models, such as the Topcolor-assisted Technicolor (TC2) Model and the Minimal Supersymmetric Standard Model (MSSM). Many studies have been performed and shown that the existence of FC top quark interactions in various new physics models can significantly enhance the branching ratios of the rare top quark decays [8–10] and the cross sections of the top-charm production at hadron colliders [11–13] and linear colliders [14–17]. Such FC interactions can also significantly influence other FC processes involving top quark [18,19]. Due to the fact that different new physics models predict different orders of enhancement, the measurement of these FC top quark processes at the LHC will provide a unique way to distinguish these models. In the LHT model, one of the important ingredients of the mirror sector is the existence of CKM-like unitary mixing matrices. These mirror mixing matrices parameterize the FC interactions between the SM fermions and the mirror fermions. Such new FC interactions also have a very different pattern from ones present in the SM and can have significant contributions to some FC processes. The impact of the FC interactions in the LHT model on the K, B, D systems was firstly studied in [20]. Then the group of Blanke et al. have done an extensive study about the effect of the FC transitions in the LHT model on the meson systems [21–24]. Specially, Ref. [22] has extended the previous LHT flavor analyses to included all prominent rare K and B decays and a collection of Feynman rules including v^2/f^2 contributions is given for the first time which is very useful for other phenomenological studies about the LHT model. Furthermore, the effect of FC couplings in the LHT model on the lepton flavor violating decays was studied in Ref. [25]. The FC couplings between the SM fermions and the mirror fermions can also make the loop-level contributions to the tcV $(V = \gamma, Z, g)$ couplings. Such contributions can significantly enhance the branching ratios of the rare top quark decays $t \to cV$ [10] and the production rate of the process $eq \to et$ [18]. The FC couplings tcV can also make contributions to the FC top-charm quark production. We have systematically studied the top-charm quark production at the International Linear Collider (ILC) and found that these processes can open an ideal window to probe the LHT model [26]. With the running of LHC, people will pay more attention to the study about LHC. In this paper, we study the top-charm production at the LHC in the framework of the LHT model. On the other hand, the single top quark can also be produced associated with a SM neutral gauge boson via the FC couplings tcV, these processes are also studied in this paper.

This paper is organized as follows. In Section 2, we briefly review the LHT model. Section 3 presents the detailed calculation of the cross sections for the $t\bar{c}$ and tV production processes at the LHC. The numerical results are shown in Section 4. We present conclusions and summaries in the last section.

2. A brief review of the LHT model

The LHT model was introduced in paper [6] and the main features of the LHT model have been reviewed in paper [22] very well. The LH model embeds the electroweak sector of the SM in an $SU(5)/SO(5)$ non-linear sigma model. It begins with a global $SU(5)$ symmetry with a locally gauged sub-group $[SU(2) \times U(1)]^2$. The $SU(5)$ symmetry is spontaneously broken down to $SO(5)$ via a VEV of order f. At the same time, the $[SU(2) \times U(1)]^2$ gauge symmetry is broken to its diagonal subgroup $SU(2)_L \times U(1)_Y$ which is identified as the SM electroweak gauge group. From the $SU(5)/SO(5)$ breaking, there arise 14 Nambu–Goldstone bosons which

are described by the matrix Π, given explicitly by

$$\Pi = \begin{pmatrix} -\frac{\omega^0}{2} - \frac{\eta}{\sqrt{20}} & -\frac{\omega^+}{\sqrt{2}} & -i\frac{\pi^+}{\sqrt{2}} & -i\phi^{++} & -i\frac{\phi^+}{\sqrt{2}} \\ -\frac{\omega^-}{\sqrt{2}} & \frac{\omega^0}{2} - \frac{\eta}{\sqrt{20}} & \frac{v+h+i\pi^0}{2} & -i\frac{\phi^+}{\sqrt{2}} & \frac{-i\phi^0+\phi^P}{\sqrt{2}} \\ i\frac{\pi^-}{\sqrt{2}} & \frac{v+h-i\pi^0}{2} & \sqrt{4/5}\eta & -i\frac{\pi^+}{\sqrt{2}} & \frac{v+h+i\pi^0}{2} \\ i\phi^{--} & i\frac{\phi^-}{\sqrt{2}} & i\frac{\pi^-}{\sqrt{2}} & -\frac{\omega^0}{2} - \frac{\eta}{\sqrt{20}} & -\frac{\omega^-}{\sqrt{2}} \\ i\frac{\phi^-}{\sqrt{2}} & \frac{i\phi^0+\phi^P}{\sqrt{2}} & \frac{v+h-i\pi^0}{2} & -\frac{\omega^+}{\sqrt{2}} & \frac{\omega^0}{2} - \frac{\eta}{\sqrt{20}} \end{pmatrix}. \tag{1}$$

Here, $H = (-i\pi^+\sqrt{2}, (v + h + i\pi^0)/2)^T$ plays the role of the SM Higgs doublet, i.e. h is the usual Higgs field, $v = 246$ GeV is the Higgs VEV, and $\pi^\pm, \pi^0$ are the Goldstone bosons associated with the spontaneous symmetry breaking $SU(2)_L \times U(1)_Y \to U(1)_{em}$. The fields η and ω are additional Goldstone bosons eaten by heavy gauge bosons when the $[SU(2) \times U(1)]^2$ gauge group is broken down to $SU(2)_L \times U(1)_Y$. The field Φ is a physical scalar triplet with

$$\Phi = \begin{pmatrix} -i\phi^{++} & -i\frac{\phi^+}{\sqrt{2}} \\ -i\frac{\phi^+}{\sqrt{2}} & \frac{-i\phi^0+\phi^P}{\sqrt{2}} \end{pmatrix}. \tag{2}$$

Its mass is given by

$$m_\Phi = \sqrt{2} m_H \frac{f}{v}, \tag{3}$$

with m_H being the mass of the SM Higgs scalar.

In the LHT model, a T-parity discrete symmetry is introduced to make the model consistent with the electroweak precision data. Under the T-parity, the fields Φ, ω, and η are odd, and the SM Higgs doublet H is even.

For the gauge group $[SU(2) \times U(1)]^2$, there are eight gauge bosons, $W_1^{a\mu}, B_1^\mu, W_2^{a\mu}, B_2^\mu$ $(a = 1, 2, 3)$. A natural way to define the action of T-parity on the gauge fields is

$$W_1^a \Leftrightarrow W_2^a, \qquad B_1 \Leftrightarrow B_2. \tag{4}$$

An immediate consequence of this definition is that the gauge couplings of the two $SU(2) \times U(1)$ factors have to be equal.

The gauge boson T-parity eigenstates are given by

$$W_L^a = \frac{W_1^a + W_2^a}{\sqrt{2}}, \qquad B_L = \frac{B_1 + B_2}{\sqrt{2}} \quad \text{(T-even)}, \tag{5}$$

$$W_H^a = \frac{W_1^a - W_2^a}{\sqrt{2}}, \qquad B_H = \frac{B_1 - B_2}{\sqrt{2}} \quad \text{(T-odd)}. \tag{6}$$

From the first step of symmetry breaking $[SU(2) \times U(1)]^2 \to SU(2)_L \times U(1)_Y$, the T-odd heavy gauge bosons acquire masses. The masses of the T-even gauge bosons are generated only through the second step of symmetry breaking $SU(2)_L \times U(1)_Y \to U(1)_{em}$. Finally, the mass eigenstates are given at order $O(v^2/f^2)$ by

$$W_L^\pm = \frac{W_L^1 \mp i W_L^2}{\sqrt{2}}, \qquad W_H^\pm = \frac{W_H^1 \mp i W_H^2}{\sqrt{2}},$$

$$Z_L = \cos\theta_W W_L^3 - \sin\theta_W B_L, \qquad Z_H = W_H^3 + x_H \frac{v^2}{f^2} B_H,$$

$$A_L = \sin\theta_W W_L^3 + \cos\theta_W B_L, \qquad A_H = -x_H \frac{v^2}{f^2} W_H^3 + B_H, \tag{7}$$

where θ_W is the usual weak mixing angle and

$$x_H = \frac{5gg'}{4(5g^2 - g'^2)}, \tag{8}$$

with g, g' being the corresponding coupling constants of $SU(2)_L$ and $U(1)_Y$. The masses of the T-odd gauge bosons are given by

$$M_{Z_H} \equiv M_{W_H} = fg\left(1 - \frac{v^2}{8f^2}\right), \qquad M_{A_H} = \frac{fg'}{\sqrt{5}}\left(1 - \frac{5v^2}{8f^2}\right). \tag{9}$$

The masses of the T-even gauge bosons are given by

$$M_{W_L} = \frac{gv}{2}\left(1 - \frac{v^2}{12f^2}\right), \qquad M_{Z_L} = \frac{gv}{2\cos\theta_W}\left(1 - \frac{v^2}{12f^2}\right), \qquad M_{A_L} = 0. \tag{10}$$

A consistent and phenomenologically viable implementation of T-parity in the fermion sector requires the introduction of mirror fermions. The T-even fermion section consists of the SM quarks, leptons and an additional heavy quark T_+. The T-odd fermion sector consists of three generations of mirror quarks and leptons and an additional heavy quark T_-. Only the mirror quarks (u_H^i, d_H^i) are involved in this paper. The mirror quarks get masses

$$\begin{aligned} m_{H_i}^u &= \sqrt{2}\kappa_i f\left(1 - \frac{v^2}{8f^2}\right) \equiv m_{H_i}\left(1 - \frac{v^2}{8f^2}\right), \\ m_{H_i}^d &= \sqrt{2}\kappa_i f \equiv m_{H_i}, \end{aligned} \tag{11}$$

where the Yukawa couplings κ_i can in general depend on the fermion species i.

The mirror fermions induce a new flavor structure and there are four CKM-like unitary mixing matrices in the mirror fermion sector:

$$V_{H_u}, \quad V_{H_d}, \quad V_{H_l}, \quad V_{H_\nu}. \tag{12}$$

These mirror mixing matrices are involved in the FC interactions between the SM fermions and the T-odd mirror fermions which are mediated by the T-odd heavy gauge bosons or the Goldstone bosons. V_{H_u} and V_{H_d} satisfy the relation

$$V_{H_u}^\dagger V_{H_d} = V_{\rm CKM}. \tag{13}$$

We parameterize the V_{H_d} with three angles $\theta_{12}^d, \theta_{23}^d, \theta_{13}^d$ and three phases $\delta_{12}^d, \delta_{23}^d, \delta_{13}^d$

$$V_{H_d} = \begin{pmatrix} c_{12}^d c_{13}^d & s_{12}^d c_{13}^d e^{-i\delta_{12}^d} & s_{13}^d e^{-i\delta_{13}^d} \\ -s_{12}^d c_{23}^d e^{i\delta_{12}^d} - c_{12}^d s_{23}^d s_{13}^d e^{i(\delta_{13}^d - \delta_{23}^d)} & c_{12}^d c_{23}^d - s_{12}^d s_{23}^d s_{13}^d e^{i(\delta_{13}^d - \delta_{12}^d - \delta_{23}^d)} & s_{23}^d c_{13}^d e^{-i\delta_{23}^d} \\ s_{12}^d s_{23}^d e^{i(\delta_{12}^d + \delta_{23}^d)} - c_{12}^d c_{23}^d s_{13}^d e^{i\delta_{13}^d} & -c_{12}^d s_{23}^d e^{i\delta_{23}^d} - s_{12}^d c_{23}^d s_{13}^d e^{i(\delta_{13}^d - \delta_{12}^d)} & c_{23}^d c_{13}^d \end{pmatrix}. \tag{14}$$

The matrix V_{H_u} is then determined through $V_{H_u} = V_{H_d} V_{\rm CKM}^\dagger$. As in the case of the CKM matrix the angles θ_{ij}^d can all be made to lie in the first quadrant with $0 \leqslant \delta_{12}^d, \delta_{23}^d, \delta_{13}^d < 2\pi$.

3. The calculation of the cross sections for the $t\bar{c}$ and tV productions in the LHT model at the LHC

3.1. The loop-level FC couplings tcV in the LHT model

As we have mentioned above, in the LHT model there are FC interactions between the SM fermions and the T-odd mirror fermions which are mediated by the T-odd heavy gauge bosons (A_H, Z_H, $W_H^{\pm}$) or Goldstone bosons ($\eta, \omega^0, \omega^{\pm}$). The relevant Feynman rules can be found in Ref. [22]. With these FC couplings, the loop-level FC couplings tcV can be induced and the relevant Feynman diagrams are shown in Fig. 1.

Here we use the method introduced in Ref. [11] to obtain the effective vertex $tcZ(\gamma)$ firstly. Such method can greatly simplify our calculations since it avoids repetition of the evaluation of a same loop-corrected vertex in different places, or in different processes. As we know, each diagram in Fig. 1 actually contains ultraviolet divergence. Because there is no corresponding tree-level tcV coupling to absorb these divergences, the divergences just cancel each other and the total effective tcV couplings are finite as they should be. The effective one loop-level couplings tcV can be directly calculated based on Fig. 1 and their explicit forms, $\Gamma^{\mu}_{tc\gamma}(p_t, p_c)$, $\Gamma^{\mu}_{tcZ}(p_t, p_c)$ and $\Gamma^{\mu}_{tcg}(p_t, p_c)$, are given in Appendix A.

With the FC couplings tcV, the top-charm quarks can be produced via gluon–gluon collision or $q\bar{q}$ collision. On the other hand, single top quark can also be produced associated with a SM gauge boson via charm–gluon collision. We will study these processes in the following.

3.2. The $t\bar{c}$ production in the LHT model at the LHC

In the LHT model, the existence of the FC couplings tcV can induce the subprocesses $gg \to t\bar{c}$ and $q\bar{q} \to t\bar{c}$ at loop-level. The corresponding Feynman diagrams are shown in Fig. 2, and the production amplitudes are

$$\begin{aligned}
M_A &= ig_s f^{abc} G(p_1+p_2,0)\bar{u}_t^i(p_3)\Gamma_{tcg}^{\mu aij}(p_3,-p_4)\big[(p_1-p_2)_\mu \epsilon^c(p_1)\cdot\epsilon^b(p_2) \\
&\quad + 2p_2\cdot\epsilon^c(p_1)\epsilon_\mu^b(p_2) - 2p_1\cdot\epsilon^b(p_2)\epsilon_\mu^c(p_1)\big]v_{\bar{c}}^j(p_4), \qquad (15)\\
M_B &= -g_s T^{bjk} G(p_3-p_1,m_c)\bar{u}_t^i(p_3)\Gamma_{tcg}^{\mu aij}(p_3,p_3-p_1)\epsilon_\mu^a(p_1) \\
&\quad \times(\not{p}_3-\not{p}_1+m_c)\not{\epsilon}^b(p_2)v_{\bar{c}}^k(p_4), \qquad (16)\\
M_C &= -g_s T^{aij} G(p_3-p_1,m_t)\bar{u}_t^i(p_3)\not{\epsilon}^a(p_1)(\not{p}_3-\not{p}_1+m_t) \\
&\quad \times\Gamma_{tcg}^{\mu bjk}(p_3-p_1,-p_4)\epsilon_\mu^b(p_2)v_{\bar{c}}^k(p_4), \qquad (17)\\
M_D &= g_s T^{alj} G(p_1+p_2,0)\bar{u}_t^i(p_3)\Gamma_{tcg}^{\mu aik}(p_3,-p_4)v_{\bar{c}}^k(p_4)\bar{v}_{\bar{q}}^l(p_2)\gamma_\mu u_q^j(p_1), \qquad (18)\\
M_E &= g_s T^{alk} G(p_3-p_1,0)\bar{u}_t^i(p_3)\Gamma_{tcg}^{\mu aij}(p_3,p_1)u_c^j(p_1)\bar{v}_{\bar{c}}^l(p_2)\gamma_\mu v_{\bar{c}}^k(p_4). \qquad (19)
\end{aligned}$$

Here p_1, p_2 are the momenta of the incoming states, and p_3, p_4 are the momenta of the outgoing final states top quark and anti-charm quarks, respectively. We also define $G(p,m)$ as $\frac{1}{p^2-m^2}$. In our calculation, we use an effective vertex method introduced in paper [11] which can greatly simplify our calculations since it avoids repetition of the evaluation of a same loop-corrected vertex in different places, or in different processes.

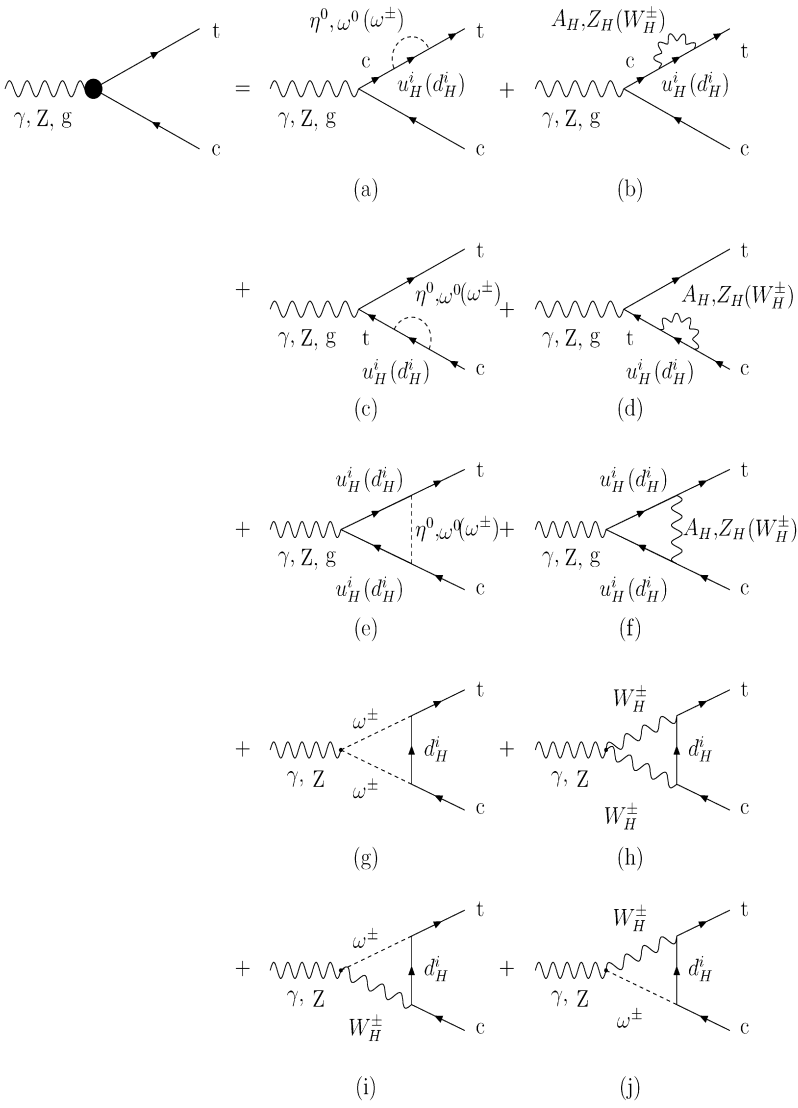

Fig. 1. One-loop contributions of the LHT model to the tcV couplings.

3.3. The tV production in the LHT model at the LHC

The FC couplings tcV can also induce the FC single top quark production $cg \to tV$ at hadron colliders. The corresponding Feynman diagrams are shown in Fig. 3, and the production amplitudes can be written as

$$M_F^\gamma = -\frac{2e}{3} G(p_1+p_2, m_t)\bar{u}_t^i(p_3)\not{\epsilon}(p_4)(\not{p}_1+\not{p}_2+m_t) \times \Gamma_{tcg}^{\mu a i j}(p_1+p_2, p_1)\epsilon_\mu^a(p_2)u_c^j(p_1), \tag{20}$$

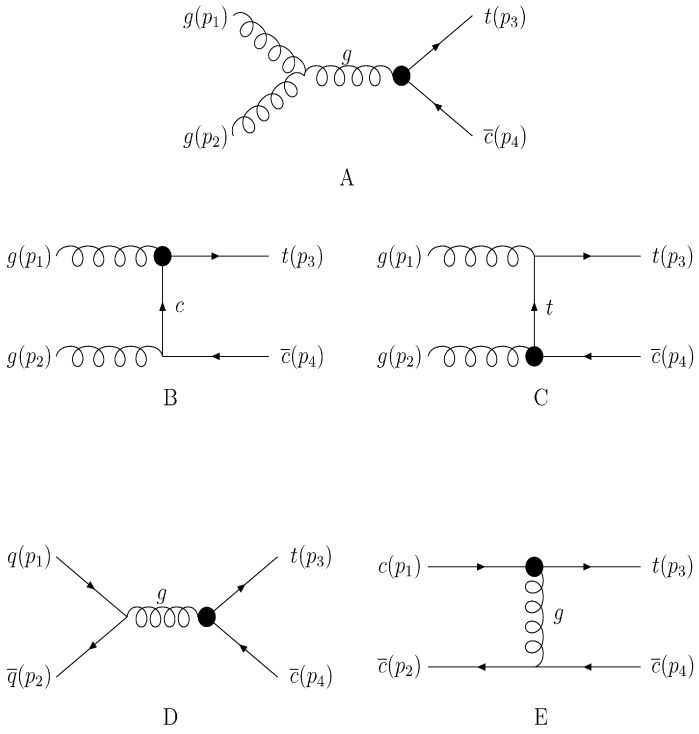

Fig. 2. The Feynman diagrams of the subprocesses $gg(q\bar{q}) \to t\bar{c}$ in the LHT model. The blob represents the LHT loop contributions illustrated in Fig. 1.

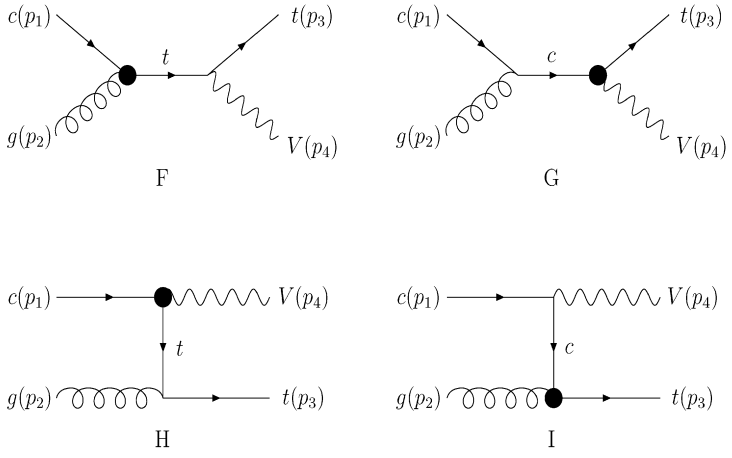

Fig. 3. The Feynman diagrams of the subprocesses $cg \to tV$ $(V = \gamma, Z, g)$ in the LHT model. The blob represents the LHT loop contributions illustrated in Fig. 1.

$$M_F^Z = -\frac{g}{\cos\theta_W} G(p_1+p_2, m_t)\bar{u}_t^i(p_3)\not{\epsilon}(p_4)\left[\left(\frac{1}{2}-\frac{2}{3}\sin^2\theta_W\right)P_L - \frac{2}{3}\sin^2\theta_W P_R\right]$$
$$\times (\not{p}_1+\not{p}_2+m_t)\Gamma_{tcg}^{\mu aij}(p_1+p_2, p_1)\epsilon_\mu^a(p_2)u_c^j(p_1), \tag{21}$$

$$M_F^g = -g_s T^{bil} G(p_1+p_2, m_t)\bar{u}_t^i(p_3)\not{\epsilon}^b(p_4)(\not{p}_1+\not{p}_2+m_t)$$
$$\times \Gamma_{tcg}^{\mu alj}(p_1+p_2, p_1)\epsilon_\mu^a(p_2)u_c^j(p_1), \tag{22}$$

$$M_G^\gamma = -g_s T^{aij} G(p_1+p_2, m_c)\bar{u}_t^i(p_3)\Gamma_{tc\gamma}^\mu(p_3, p_3+p_4)$$
$$\times \epsilon_\mu(p_4)(\not{p}_1+\not{p}_2+m_c)\not{\epsilon}^a(p_2)u_c^j(p_1), \tag{23}$$

$$M_G^Z = -g_s T^{aij} G(p_1+p_2, m_c)\bar{u}_t^i(p_3)\Gamma_{tcZ}^\mu(p_3, p_3+p_4)$$
$$\times \epsilon_\mu(p_4)(\not{p}_1+\not{p}_2+m_c)\not{\epsilon}^a(p_2)u_c^j(p_1), \tag{24}$$

$$M_G^g = -g_s T^{alj} G(p_1+p_2, m_c)\bar{u}_t^i(p_3)\Gamma_{tcg}^{\mu bil}(p_3, p_3+p_4)$$
$$\times \epsilon_\mu^b(p_4)(\not{p}_1+\not{p}_2+m_c)\not{\epsilon}^a(p_2)u_c^j(p_1), \tag{25}$$

$$M_H^\gamma = -g_s T^{aij} G(p_3-p_2, m_t)\bar{u}_t^i(p_3)\not{\epsilon}^a(p_2)(\not{p}_3-\not{p}_2+m_t)$$
$$\times \Gamma_{tc\gamma}^\mu(p_1-p_4, p_1)\epsilon_\mu(p_4)u_c^j(p_1), \tag{26}$$

$$M_H^Z = -g_s T^{aij} G(p_3-p_2, m_t)\bar{u}_t^i(p_3)\not{\epsilon}^a(p_2)(\not{p}_3-\not{p}_2+m_t)$$
$$\times \Gamma_{tcZ}^\mu(p_1-p_4, p_1)\epsilon_\mu(p_4)u_c^j(p_1), \tag{27}$$

$$M_H^g = -g_s T^{ail} G(p_3-p_2, m_t)\bar{u}_t^i(p_3)\not{\epsilon}^a(p_2)(\not{p}_3-\not{p}_2+m_t)$$
$$\times \Gamma_{tcg}^{\mu blj}(p_1-p_4, p_1)\epsilon_\mu^b(p_4)u_c^j(p_1), \tag{28}$$

$$M_I^\gamma = -\frac{2e}{3} G(p_3-p_2, m_c)\bar{u}_t^i(p_3)\Gamma_{tcg}^{\mu aij}(p_3, p_3-p_2)$$
$$\times \epsilon_\mu^a(p_2)(\not{p}_3-\not{p}_2+m_c)\not{\epsilon}(p_4)u_c^j(p_1), \tag{29}$$

$$M_I^Z = -\frac{g}{\cos\theta_W} G(p_3-p_2, m_c)\bar{u}_t^i(p_3)\Gamma_{tcg}^{\mu aij}(p_3, p_3-p_2)\epsilon_\mu^a(p_2)(\not{p}_3-\not{p}_2+m_c)\not{\epsilon}(p_4)$$
$$\times \left[\left(\frac{1}{2}-\frac{2}{3}\sin^2\theta_W\right)P_L - \frac{2}{3}\sin^2\theta_W P_R\right]u_c^j(p_1), \tag{30}$$

$$M_I^g = -g_s T^{blj} G(p_3-p_2, m_c)\bar{u}_t^i(p_3)\Gamma_{tcg}^{\mu ail}(p_3, p_3-p_2)$$
$$\times \epsilon_\mu^a(p_2)(\not{p}_3-\not{p}_2+m_c)\not{\epsilon}^b(p_4)u_c^j(p_1). \tag{31}$$

With the above production amplitudes, we can directly obtain the cross sections $\hat{\sigma}_{ij}(\hat{s})$ of the subprocesses $gg \to t\bar{c}$, $q\bar{q} \to t\bar{c}$ and $cg \to tV$, where $\hat{s} = (p_1+p_2)^2$. The hadronic cross sections at the hadron colliders can be obtained by folding the cross sections of the subprocesses with the parton distribution functions: $f_i^A(x_1, Q)$and $f_j^B(x_2, Q)$, which is given by

$$\sigma(s) = \sum_{ij}\int dx_1\, dx_2 \left[f_i^A(x_1, Q) f_j^B(x_2, Q) + f_i^B(x_1, Q) f_j^A(x_2, Q)\right]\hat{\sigma}^{ij}\left(\hat{s}, \alpha_s(\mu)\right). \tag{32}$$

Thereinto, Q is the factorization scale, μ is the renormalization scale, $\sqrt{s}$ is the center-of-mass (c.m.) energy of the hadron colliders. Here we used the parton distribution functions that were given by CTEQ6L [27].

To obtain numerical results of the cross sections, we calculate the amplitudes numerically by using the method of Ref. [28], instead of calculating the square of the production amplitudes analytically. This greatly simplifies our calculations.

4. The numerical results of the cross sections

There are several free parameters in the LHT model which are involved in the production amplitudes. They are the breaking scale f, the mirror quark masses m_{H_i} $(i = 1, 2, 3)$ (here we have ignored the mass difference between the up-type mirror quarks and the down-type mirror quarks), and 6 parameters (θ^d_{12}, θ^d_{13}, θ^d_{23}, δ^d_{12}, δ^d_{13}, δ^d_{23}) which are related to the mixing matrix V_{H_d}. In Refs. [20–22], the constraints on the mass spectrum of the mirror fermions have been investigated from the analysis of neutral meson mixing in the K, B and D systems. They found that a TeV scale GIM suppression is necessary for a generic choice of V_{H_d}. However, there are regions of parameter space where are only very loose constraints on the mass spectrum of the mirror fermions. Here we calculate the cross sections based on the two scenarios for the structure of the matrix V_{H_d}, as in Ref. [10]. i.e.,

$$\begin{aligned}&\text{Case I:} \quad V_{H_d} = 1, \quad V_{H_u} = V^\dagger_{\text{CKM}},\\ &\text{Case II:} \quad s^d_{23} = 1/\sqrt{2}, \quad s^d_{12} = s^d_{13} = 0, \quad \delta^d_{12} = \delta^d_{23} = \delta^d_{13} = 0.\end{aligned}$$

In both cases, the constraints on the mass spectrum of the mirror fermions are very relaxed. On the other hand, the Ref. [29] has shown that the experimental bounds on four-fermi interactions involving SM fields provide an upper bound on the mirror fermion masses and this yields $m_{H_i} \leqslant 4.8 f^2$. In our calculation, we also consider such constraint. For the breaking scale f, we take two typical values: 500 GeV and 1000 GeV.

To get the numerical results of the cross sections, we should also fix some parameters in the SM as $m_t = 174.2$ GeV, $m_c = 1.25$ GeV, $s^2_W = 0.23$, $M_Z = 91.87$ GeV, $\alpha_e = 1/128$, $\alpha_s = 0.1$, and $v = 246$ GeV [30]. On the other hand, taking account of the detector acceptance, we have taken the basic cuts on the transverse momenta (p_T) and the pseudo-rapidities (η) for the final state particles

$$p_T \geqslant 20\ \text{GeV}, \qquad |\eta| \leqslant 2.5.$$

The numerical results of the cross sections for the $t\bar{c}$ and tV productions at the LHC are summarized in Figs. 4–5, and here the anti-top quark ($\bar{t}$) production is also included in our calculation. The numerical results for Case I are shown in Fig. 4. In Case I, the mixing in the down type gauge and Goldstone boson interactions is absent. In this case, there are no constraints on the mirror quark masses at one loop-level from the K and B systems and the constraints come only from the D system. The constraints on the mass of the third generation mirror quark are very weak. On the other hand, the constraint $m_{H_i} \leqslant 4.8 f^2$ should also be considered. So we take m_{H_3} to vary in the range of 500–1200 GeV for $f = 500$ GeV and 500–4800 GeV for $f = 1000$ GeV, and fix $m_{H_1} = m_{H_2} = 500$ GeV. We can see from Fig. 4 that all the cross sections rise very fast with the m_{H_3} increasing. This is because the couplings between the mirror quarks and the SM quarks are proportional to the mirror quark masses. The cross sections are insensitive to the scale f. The reason is that the masses of the heavy gauge bosons and the mirror quarks, M_{V_H} and m_{H_i}, are proportional to f but the production amplitudes are represented in the form of m_{H_i}/M_{V_H} which cancels the effect of f. Among all the processes, the process $pp \to t\bar{c}$ possesses the largest cross section. With $f = 1000$ GeV and heavy mirror quarks, the cross section

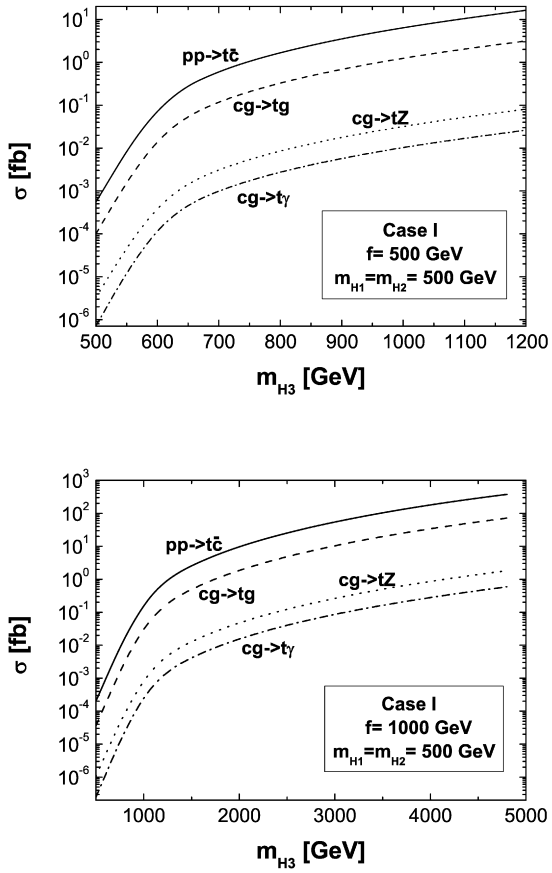

Fig. 4. The cross sections of the processes $pp \to t\bar{c}$ and $pp \to tV$ in the LHT model at the LHC for Case I, as a function of M_{H_3}. Here we fix $m_{H_1} = m_{H_2} = 500$ GeV and take $f = 500$ GeV, $f = 1000$ GeV, respectively.

of $pp \to t\bar{c}$ can reach the level of 10^2 fb. The cross sections of $pp \to t\gamma(Z)$ are much smaller than that of $pp \to t\bar{c}$ and their cross sections can only reach 10^{-1} fb with relative large value of mirror quark masses. On the other hand, we find that the process $pp \to tg$ can also have a sizeable cross section and a large number of tg events can be produced at the LHC. For Case II, the dependence of the cross sections on m_{H_3} is presented in Fig. 5. In this case, the constraints from the K and B systems are also very weak. Compared to Case I, the mixing between the second and third generations is enhanced with the choice of a bigger mixing angle s_{23}^d. The dependence of the cross sections on the free parameters is similar to that in Case I. Here, we also consider the other constraint $m_{H_i} \leqslant 4.8 f^2$. In this case, the cross sections can also reach a sizeable level. Specially, the processes $pp \to t\bar{c}$ and $pp \to tg$ benefit from their large cross sections.

5. The discussions of the potential to observe the FC $t\bar{c}$ and tV productions at the LHC

The potential to observe the FC $t\bar{c}$ and tV productions at the LHC strongly depends on the backgrounds. To reduce the large QCD backgrounds at the LHC, the search for these processes

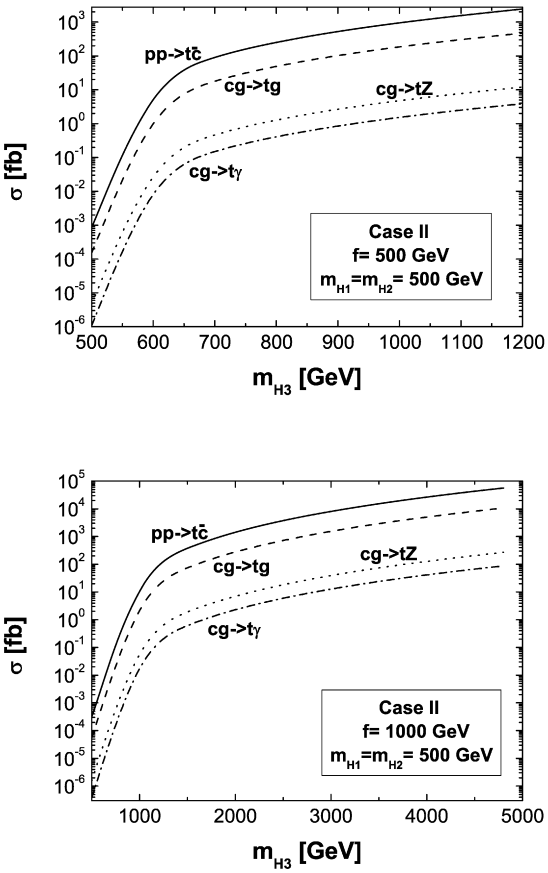

Fig. 5. The cross sections of the processes $pp \to t\bar{c}$ and $pp \to tV$ in the LHT model at the LHC for Case II, as a function of M_{H_3}. Here we fix $m_{H_1} = m_{H_2} = 500$ GeV and take $f = 500$ GeV, $f = 1000$ GeV, respectively.

must be performed in the decay channels $W \to l\bar{\nu}_l$ $(l = e, \mu)$ for the W boson, $Z \to l^+l^-$ for the Z boson. For any of these FC processes, top quark reconstruction is required to extract the signal from its background. The observability of the single-top quark production at the LHC has been intensively studied in the effective Lagrangian approach for $t \to cV$ $(V = \gamma, Z, g)$ [31], for $pp \to tV + X$ [32,33], and for $pp \to t\bar{c} + X$ [32]. In order to see the potential to observe the FC $t\bar{c}$ and tV productions in various new physics models at the LHC, in Table 1, we show the maximal predictions for these processes in the MSSM, the TC2 model and the LHT model at the LHC. The LHC sensitivities are also listed in the last column of Table 1. Comparing the maximal predictions in the MSSM model, TC2 model and LHT model at the LHC with the LHC sensitivities, we find that it is possible to observe the FC processes $t\bar{c}$ and tV at the LHC based the ideal prediction of TC2 model and LHT model. But it is very hard to find the MSSM signal via these processes. If these FC processes are observed at the LHC, more precise measurement more careful theoretical analysis are needed in order to distinguish different new physics models. If these FC processes are not be observed, we can give a up-limit about the mirror quark masses at least.

Table 1
The maximal predictions (in fb) for $pp \to t\bar{c}$ and $pp \to tV$ processes in the MSSM [11], TC2 model [13] and LHT model. The LHC sensitivities listed are for 100 fb^{-1} integrated luminosity [32,33]. The predictions in the MSSM model are based on two cases ($\delta_{LL} \neq 0$ and $\delta_{LR} \neq 0$) with all constraints.

Processes	MSSM $\delta_{LL} \neq 0$	MSSM $\delta_{LR} \neq 0$	TC2	LHT for Case I	LHT for Case II	LHC sensitivity at 3σ level
$pp \to t\bar{c}$	$O(10^2)$	$O(10^2)$	$O(10^4)$	$O(10^2)$	$O(10^4)$	1500
$pp \to tg$	$O(10)$	$O(10^2)$	$O(10^3)$	$O(10^1)$	$O(10^4)$	1500
$pp \to t\gamma$	$O(10^{-1})$	$O(1)$	$O(10)$	$O(10^{-1})$	$O(10^1)$	5
$pp \to tZ$	$O(1)$	$O(1)$	$O(10^2)$	$O(1)$	$O(10^2)$	35

6. Conclusions and summaries

In this paper, we study some interesting FC single-top quark production processes, $pp \to t\bar{c}$ and $pp \to tV$, at the LHC in the framework of the LHT model. We can conclude that: (1) All the cross sections of these processes strongly depend on the mirror quark masses and the cross sections increase sharply with the mirror quark masses increasing. (2) The cross sections are insensitive to the scale f. (3) The cross section of the process $pp \to t\bar{c}$ is the largest one which can reach tens pb in some ideal case. The process $pp \to tg$ also has a sizeable cross section but the cross sections of $pp \to t\gamma(Z)$ are much smaller. With the running of the LHC, it should have ability to probe the LHT model via these FC single-top quark production processes.

Acknowledgements

We would thank Junjie Cao for useful discussions and providing the calculation programs. This work is supported by the National Natural Science Foundation of China under Grant Nos. 10775039, 10575029 and 10505007.

Appendix A. The explicit expressions of the effective tcV couplings

The effective tcV couplings $\Gamma^{\mu}_{tc\gamma}$, Γ^{μ}_{tcZ}, Γ^{μ}_{tcg} can be directly calculated based on Fig. 1, and they can be represented in form of 2-point and 3-point standard functions B_0, B_1, C_{ij}. Due to $m_t \gg m_c$, we have safely ignored the terms m_c/m_t in the calculation. On the other hand, the higher order v^2/f^2 terms in the masses of new gauge bosons and in the Feynman rules are also ignored. $\Gamma^{\mu}_{tc\gamma}$, Γ^{μ}_{tcZ}, Γ^{μ}_{tcg} depend on the momenta of top quark and charm quark(p_t, p_c). Here p_t is outgoing and p_c is incoming. The explicit expressions of them are

$$\begin{aligned}
\Gamma^{\mu aij}_{tcg}(p_t, p_c) &= \Gamma^{\mu aij}_{tcg}\big(\eta^0\big) + \Gamma^{\mu aij}_{tcg}\big(\omega^0\big) + \Gamma^{\mu aij}_{tcg}\big(\omega^{\pm}\big) \\
&\quad + \Gamma^{\mu aij}_{tcg}(A_H) + \Gamma^{\mu aij}_{tcg}(Z_H) + \Gamma^{\mu aij}_{tcg}\big(W^{\pm}_H\big),
\end{aligned}$$

$$\begin{aligned}
\Gamma^{\mu aij}_{tcg}\big(\eta^0\big) &= \frac{i}{16\pi^2}\frac{g'^2}{100M^2_{A_H}}(V_{Hu})^*_{it}(V_{Hu})_{ic}m^2_{Hi}g_sT^{aij} \\
&\quad \times \Big\{\big[B_0(-p_t, m_{Hi}, 0) - B_0(-p_c, m_{Hi}, 0) + B_1(-p_t, m_{Hi}, 0) \\
&\quad + 2C^a_{24} - 2p_t \cdot p_c\big(C^a_{12} + C^a_{23}\big) + m^2_t\big(C^a_{21} + C^a_{11} + C^a_0\big) - m^2_{Hi}C^a_0\big]\gamma^{\mu}P_L \\
&\quad + \big[-2m_t\big(C^a_{21} + 2C^a_{11} + C^a_0\big)\big]p^{\mu}_t P_L + \big[2m_t\big(C^a_{23} + 2C^a_{12}\big)\big]p^{\mu}_c P_L\Big\},
\end{aligned}$$

$$\Gamma_{tcg}^{\mu aij}(\omega^0) = \frac{i}{16\pi^2}\frac{g^2}{4M_{Z_H}^2}(V_{Hu})_{it}^*(V_{Hu})_{ic}m_{Hi}^2 g_s T^{aij} \times \{[B_0(-p_t, m_{Hi}, 0) - B_0(-p_c, m_{Hi}, 0) + B_1(-p_t, m_{Hi}, 0) + 2C_{24}^b - 2p_t \cdot p_c(C_{12}^b + C_{23}^b) + m_t^2(C_{21}^b + C_{11}^b + C_0^b) - m_{Hi}^2 C_0^b]\gamma^\mu P_L + [-2m_t(C_{21}^b + 2C_{11}^b + C_0^b)]p_t^\mu P_L + [2m_t(C_{23}^b + 2C_{12}^b)]p_c^\mu P_L\},$$

$$\Gamma_{tcg}^{\mu aij}(\omega^\pm) = \frac{i}{16\pi^2}\frac{g^2}{2M_{W_H}^2}(V_{Hu})_{it}^*(V_{Hu})_{ic}m_{Hi}^2 g_s T^{aij} \times \{[B_0(-p_t, m_{Hi}, 0) - B_0(-p_c, m_{Hi}, 0) + B_1(-p_t, m_{Hi}, 0) + 2C_{24}^c - 2p_t \cdot p_c(C_{12}^c + C_{23}^c) + m_t^2(C_{21}^c + C_{11}^c + C_0^c) - m_{Hi}^2 C_0^c]\gamma^\mu P_L + [-2m_t(C_{21}^c + 2C_{11}^c + C_0^c)]p_t^\mu P_L + [2m_t(C_{23}^c + 2C_{12}^c)]p_c^\mu P_L\},$$

$$\Gamma_{tcg}^{\mu aij}(A_H) = \frac{i}{16\pi^2}\frac{g'^2}{50}(V_{Hu})_{it}^*(V_{Hu})_{ic}g_s T^{aij} \times \{[B_1(-p_t, m_{Hi}, M_{A_H}) + 2C_{24}^d - 2p_t \cdot p_c(C_{11}^d + C_{23}^d) + m_t^2(C_{21}^d + C_{11}^d) - m_{Hi}^2 C_0^d]\gamma^\mu P_L + [-2m_t(C_{21}^d + C_{11}^d)]p_t^\mu P_L + [2m_t(C_{23}^d + C_{11}^d)]p_c^\mu P_L\},$$

$$\Gamma_{tcg}^{\mu aij}(Z_H) = \frac{i}{16\pi^2}\frac{g^2}{2}(V_{Hu})_{it}^*(V_{Hu})_{ic}g_s T^{aij} \times \{[B_1(-p_t, m_{Hi}, M_{Z_H}) + 2C_{24}^e - 2p_t \cdot p_c(C_{11}^e + C_{23}^e) + m_t^2(C_{21}^e + C_{11}^e) - m_{Hi}^2 C_0^e]\gamma^\mu P_L + [-2m_t(C_{21}^e + C_{11}^e)]p_t^\mu P_L + [2m_t(C_{23}^e + C_{11}^e)]p_c^\mu P_L\},$$

$$\Gamma_{tcg}^{\mu aij}(W_H^\pm) = \frac{i}{16\pi^2}g^2(V_{Hu})_{it}^*(V_{Hu})_{ic}g_s T^{aij} \times \{[B_1(-p_t, m_{Hi}, M_{W_H}) + 2C_{24}^f - 2p_t \cdot p_c(C_{11}^f + C_{23}^f) + m_t^2(C_{21}^f + C_{11}^f) - m_{Hi}^2 C_0^f]\gamma^\mu P_L + [-2m_t(C_{21}^f + C_{11}^f)]p_t^\mu P_L + [2m_t(C_{23}^f + C_{11}^f)]p_c^\mu P_L\}.$$

$$\Gamma_{tc\gamma}^\mu(p_t, p_c) = \Gamma_{tc\gamma}^\mu(\eta^0) + \Gamma_{tc\gamma}^\mu(\omega^0) + \Gamma_{tc\gamma}^\mu(\omega^\pm) + \Gamma_{tc\gamma}^\mu(A_H) + \Gamma_{tc\gamma}^\mu(Z_H) + \Gamma_{tc\gamma}^\mu(W_H^\pm) + \Gamma_{tc\gamma}^\mu(W_H^\pm\omega^\pm),$$

$$\Gamma_{tc\gamma}^\mu(\eta^0) = \frac{i}{16\pi^2}\frac{eg'^2}{150M_{A_H}^2}(V_{Hu})_{it}^*(V_{Hu})_{ic}m_{Hi}^2 \times \{[B_0(-p_t, m_{Hi}, 0) - B_0(-p_c, m_{Hi}, 0) + B_1(-p_t, m_{Hi}, 0) + 2C_{24}^a - 2p_t \cdot p_c(C_{12}^a + C_{23}^a) + m_t^2(C_{21}^a + C_{11}^a + C_0^a) - m_{Hi}^2 C_0^a]\gamma^\mu P_L + [-2m_t(C_{21}^a + 2C_{11}^a + C_0^a)]p_t^\mu P_L + [2m_t(C_{23}^a + 2C_{12}^a)]p_c^\mu P_L\},$$

$$\Gamma^{\mu}_{tc\gamma}(\omega^0) = \frac{i}{16\pi^2}\frac{eg^2}{6M^2_{Z_H}}(V_{Hu})^*_{it}(V_{Hu})_{ic}m^2_{Hi}$$
$$\times\{\big[B_0(-p_t,m_{Hi},0) - B_0(-p_c,m_{Hi},0) + B_1(-p_t,m_{Hi},0)$$
$$+ 2C^b_{24} - 2p_t\cdot p_c\big(C^b_{12}+C^b_{23}\big) + m^2_t\big(C^b_{21}+C^b_{11}+C^b_0\big) - m^2_{Hi}C^b_0\big]\gamma^{\mu}P_L$$
$$+\big[-2m_t\big(C^b_{21}+2C^b_{11}+C^b_0\big)\big]p^{\mu}_t P_L + \big[2m_t\big(C^b_{23}+2C^b_{12}\big)\big]p^{\mu}_c P_L\big\},$$

$$\Gamma^{\mu}_{tc\gamma}(\omega^{\pm}) = \frac{i}{16\pi^2}\frac{eg^2}{6M^2_{W_H}}(V_{Hu})^*_{it}(V_{Hu})_{ic}m^2_{Hi}$$
$$\times\big\{2\big[(B_0(-p_t,m_{Hi},0) - B_0(-p_c,m_{Hi},0) + B_1(-p_t,m_{Hi},0))$$
$$- 2C^c_{24} + 6C^g_{24} + 2p_t\cdot p_c\big(C^c_{12}+C^c_{23}\big) - m^2_t\big(C^c_{21}+C^c_{11}+C^c_0\big)$$
$$+ m^2_{Hi}C^c_0\big]\gamma^{\mu}P_L + \big[2m_t\big(C^c_{21}+2C^c_{11}+C^c_0\big) + 3m_t\big(2C^g_{21}+C^g_{11}\big)\big]p^{\mu}_t P_L$$
$$+\big[-2m_t\big(C^c_{23}+2C^c_{12}\big) - 3m_t\big(2C^g_{23}+C^g_{11}\big)\big]p^{\mu}_c P_L\big\},$$

$$\Gamma^{\mu}_{tc\gamma}(A_H) = \frac{i}{16\pi^2}\frac{eg'^2}{75}(V_{Hu})^*_{it}(V_{Hu})_{ic}$$
$$\times\big\{\big[B_1(-p_t,m_{Hi},M_{A_H}) + 2C^d_{24} - 2p_t\cdot p_c\big(C^d_{11}+C^d_{23}\big) + m^2_t\big(C^d_{21}+C^d_{11}\big)$$
$$- m^2_{Hi}C^d_0\big]\gamma^{\mu}P_L + \big[-2m_t\big(C^d_{21}+C^d_{11}\big)\big]p^{\mu}_t P_L + \big[2m_t\big(C^d_{23}+C^d_{11}\big)\big]p^{\mu}_c P_L\big\},$$

$$\Gamma^{\mu}_{tc\gamma}(Z_H) = \frac{i}{16\pi^2}\frac{eg^2}{3}(V_{Hu})^*_{it}(V_{Hu})_{ic}$$
$$\times\big\{\big[B_1(-p_t,m_{Hi},M_{Z_H}) + 2C^e_{24} - 2p_t\cdot p_c(C^e_{11}+C^e_{23}) + m^2_t\big(C^e_{21}+C^e_{11}\big)$$
$$- m^2_{Hi}C^e_0\big]\gamma^{\mu}P_L + \big[-2m_t\big(C^e_{21}+C^e_{11}\big)\big]p^{\mu}_t P_L + \big[2m_t\big(C^e_{23}+C^e_{11}\big)\big]p^{\mu}_c P_L\big\},$$

$$\Gamma^{\mu}_{tc\gamma}\big(W^{\pm}_H\big) = \frac{i}{16\pi^2}\frac{eg^2}{6}(V_{Hu})^*_{it}(V_{Hu})_{ic}$$
$$\times\big\{\big[4B_1(-p_t,m_{Hi},M_{W_H}) + 2B_0(p_c,m_{Hi},M_{W_H}) - 4C^f_{24} + 4C^h_{24}$$
$$+ 4p_t\cdot p_c\big(C^f_{11}+C^f_{23}\big) - 2m^2_t\big(C^f_{21}+C^f_{11}\big) + 2m^2_{Hi}C^f_0 + 2M^2_{W_H}C^h_0$$
$$- 4p_t\cdot p_c\big(C^h_{11}+C^h_0\big) + m^2_t\big(3C^h_{11}+C^h_0\big)\big]\gamma^{\mu}P_L$$
$$+\big[4m_t\big(C^f_{21}+C^f_{11}\big) + 2m_t\big(3C^h_{11}+2C^h_{21}+C^h_0\big)\big]p^{\mu}_t P_L$$
$$+\big[-4m_t\big(C^f_{23}+C^f_{11}\big) - 2m_t\big(2C^h_{23}+3C^h_{12}-C^h_{11}-C^h_0\big)\big]p^{\mu}_c P_L\big\},$$

$$\Gamma^{\mu}_{tc\gamma}\big(W^{\pm}_H\omega^{\pm}\big) = \frac{i}{16\pi^2}\frac{eg^2}{2}(V_{Hu})^*_{it}(V_{Hu})_{ic}$$
$$\times\big\{\big[m^2_{Hi}\big(C^i_0-C^j_0\big) + m^2_t\big(C^j_{11}+C^j_0\big)\big]\gamma^{\mu}P_L + \big[-2m_tC^j_{12}\big]p^{\mu}_c P_L\big\}.$$

$$\Gamma^{\mu}_{tcZ}(p_t,p_c) = \Gamma^{\mu}_{tcZ}\big(\eta^0\big) + \Gamma^{\mu}_{tcZ}\big(\omega^0\big) + \Gamma^{\mu}_{tcZ}\big(\omega^{\pm}\big) + \Gamma^{\mu}_{tcZ}(A_H) + \Gamma^{\mu}_{tcZ}(Z_H) + \Gamma^{\mu}_{tcZ}\big(W^{\pm}_H\big)$$
$$+ \Gamma^{\mu}_{tcZ}\big(W^{\pm}_H\omega^{\pm}\big),$$

$$\Gamma^{\mu}_{tcZ}\big(\eta^0\big) = \frac{i}{16\pi^2}\frac{g}{\cos\theta_W}\left(\frac{1}{2}-\frac{2}{3}\sin^2\theta_W\right)\frac{g'^2}{100M^2_{A_H}}(V_{Hu})^*_{it}(V_{Hu})_{ic}m^2_{Hi}$$
$$\times\big\{\big[B_0(-p_t,m_{Hi},0) - B_0(-p_c,m_{Hi},0) + B_1(-p_t,m_{Hi},0)$$

$$
\begin{aligned}
&+2C_{24}^{a}-2p_t\cdot p_c\big(C_{12}^{a}+C_{23}^{a}\big)+m_t^2\big(C_{21}^{a}+C_{11}^{a}+C_{0}^{a}\big)-m_{Hi}^2C_{0}^{a}\big]\gamma^{\mu}P_L\\
&+\big[-2m_t\big(C_{21}^{a}+2C_{11}^{a}+C_{0}^{a}\big)\big]p_t^{\mu}P_L+\big[2m_t\big(C_{23}^{a}+2C_{12}^{a}\big)\big]p_c^{\mu}P_L\big\},
\end{aligned}
$$

$$
\begin{aligned}
\Gamma_{tcZ}^{\mu}\big(\omega^0\big)=&\frac{i}{16\pi^2}\frac{g}{\cos\theta_W}\left(\frac{1}{2}-\frac{2}{3}\sin^2\theta_W\right)\frac{g^2}{4M_{Z_H}^2}(V_{Hu})_{it}^{*}(V_{Hu})_{ic}m_{Hi}^2\\
&\times\big\{\big[B_0(-p_t,m_{Hi},0)-B_0(-p_c,m_{Hi},0)+B_1(-p_t,m_{Hi},0)\\
&+2C_{24}^{b}-2p_t\cdot p_c\big(C_{12}^{b}+C_{23}^{b}\big)+m_t^2\big(C_{21}^{b}+C_{11}^{b}+C_{0}^{b}\big)-m_{Hi}^2C_{0}^{b}\big]\gamma^{\mu}P_L\\
&+\big[-2m_t\big(C_{21}^{b}+2C_{11}^{b}+C_{0}^{b}\big)\big]p_t^{\mu}P_L+\big[2m_t\big(C_{23}^{b}+2C_{12}^{b}\big)\big]p_c^{\mu}P_L\big\},
\end{aligned}
$$

$$
\begin{aligned}
\Gamma_{tcZ}^{\mu}\big(\omega^{\pm}\big)=&\frac{i}{16\pi^2}\frac{g}{\cos\theta_W}\frac{g^2}{2M_{W_H}^2}(V_{Hu})_{it}^{*}(V_{Hu})_{ic}m_{Hi}^2\\
&\times\left\{\left[\left(\frac{1}{2}-\frac{2}{3}\sin^2\theta_W\right)\big(B_0(-p_t,m_{Hi},0)-B_0(-p_c,m_{Hi},0)\right.\right.\\
&\left.+B_1(-p_t,m_{Hi},0)\big)+\left(-\frac{1}{2}+\frac{1}{3}\sin^2\theta_W\right)\big(2C_{24}^{c}-2p_t\cdot p_c\big(C_{12}^{c}+C_{23}^{c}\big)\right.\\
&\left.+m_t^2\big(C_{21}^{c}+C_{11}^{c}+C_{0}^{c}\big)-m_{Hi}^2C_{0}^{c}\big)+2\cos^2\theta_WC_{24}^{g}\right]\gamma^{\mu}P_L\\
&+\left[\left(-\frac{1}{2}+\frac{1}{3}\sin^2\theta_W\right)\big(-2m_t\big(C_{21}^{c}+2C_{11}^{c}+C_{0}^{c}\big)\big)\right.\\
&\left.+\cos^2\theta_Wm_t\big(2C_{21}^{g}+C_{11}^{g}\big)\right]p_t^{\mu}P_L+\left[2\left(-\frac{1}{2}+\frac{1}{3}\sin^2\theta_W\right)m_t\big(C_{23}^{c}+2C_{12}^{c}\big)\right.\\
&\left.-\cos^2\theta_Wm_t\big(2C_{23}^{g}+C_{11}^{g}\big)\right]p_c^{\mu}P_L\Big\},
\end{aligned}
$$

$$
\begin{aligned}
\Gamma_{tcZ}^{\mu}(A_H)=&\frac{i}{16\pi^2}\frac{g}{\cos\theta_W}\left(\frac{1}{2}-\frac{2}{3}\sin^2\theta_W\right)\frac{g'^2}{50}(V_{Hu})_{it}^{*}(V_{Hu})_{ic}\\
&\times\big\{\big[B_1(-p_t,m_{Hi},M_{A_H})+2C_{24}^{d}-2p_t\cdot p_c\big(C_{11}^{d}+C_{23}^{d}\big)+m_t^2\big(C_{21}^{d}+C_{11}^{d}\big)\\
&-m_{Hi}^2C_{0}^{d}\big]\gamma^{\mu}P_L+\big[-2m_t\big(C_{21}^{d}+C_{11}^{d}\big)\big]p_t^{\mu}P_L+\big[2m_t\big(C_{23}^{d}+C_{11}^{d}\big)\big]p_c^{\mu}P_L\big\},
\end{aligned}
$$

$$
\begin{aligned}
\Gamma_{tcZ}^{\mu}(Z_H)=&\frac{i}{16\pi^2}\frac{g}{\cos\theta_W}\left(\frac{1}{2}-\frac{2}{3}\sin^2\theta_W\right)\frac{g^2}{2}(V_{Hu})_{it}^{*}(V_{Hu})_{ic}\\
&\times\big\{\big[B_1(-p_t,m_{Hi},M_{Z_H})+2C_{24}^{e}-2p_t\cdot p_c\big(C_{11}^{e}+C_{23}^{e}\big)+m_t^2\big(C_{21}^{e}+C_{11}^{e}\big)\\
&-m_{Hi}^2C_{0}^{e}\big]\gamma^{\mu}P_L+\big[-2m_t\big(C_{21}^{e}+C_{11}^{e}\big)\big]p_t^{\mu}P_L+\big[2m_t\big(C_{23}^{e}+C_{11}^{e}\big)\big]p_c^{\mu}P_L\big\},
\end{aligned}
$$

$$
\begin{aligned}
\Gamma_{tcZ}^{\mu}\big(W_H^{\pm}\big)=&\frac{i}{16\pi^2}\frac{g}{\cos\theta_W}g^2(V_{Hu})_{it}^{*}(V_{Hu})_{ic}\\
&\times\left\{\left[\left(\frac{1}{2}-\frac{2}{3}\sin^2\theta_W\right)B_1(-p_t,m_{Hi},M_{W_H})\right.\right.\\
&+\left(-\frac{1}{2}+\frac{1}{3}\sin^2\theta_W\right)\big(2C_{24}^{f}-2p_t\cdot p_c\big(C_{11}^{f}+C_{23}^{f}\big)\right.\\
&\left.+m_t^2\big(C_{21}^{f}+C_{11}^{f}\big)-m_{Hi}^2C_{0}^{f}\big)+\frac{1}{6}\cos^2\theta_W\big(2B_0(p_c,m_{Hi},M_{W_H})+4C_{24}^{h}\right.
\end{aligned}
$$

$$
\begin{aligned}
&- 4p_t \cdot p_c\big(C_{11}^h + C_0^h\big) + m_t^2\big(3C_{11}^h + C_0^h\big) + 2M_{W_H}^2 C_0^h\Big]\gamma^\mu P_L \\
&+ \Bigg[\bigg(-\frac{1}{2} + \frac{1}{3}\sin^2\theta_W\bigg)\big(-2m_t\big(C_{21}^f + C_{11}^f\big)\big) \\
&+ \frac{1}{3}\cos^2\theta_W m_t\big(2C_{21}^h + 3C_{11}^h + C_0^h\big)\Bigg] p_t^\mu P_L \\
&+ \Bigg[2\bigg(-\frac{1}{2} + \frac{1}{3}\sin^2\theta_W\bigg) m_t\big(C_{23}^f + C_{11}^f\big) \\
&- \frac{1}{3}\cos^2\theta_W m_t\big(2C_{23}^h + 3C_{12}^h - C_{11}^h - C_0^h\big)\Bigg] p_c^\mu P_L\Bigg\},
\end{aligned}
$$

$$
\begin{aligned}
\Gamma_{tcZ}^\mu\big(W_H^\pm \omega^\pm\big) &= \frac{i}{16\pi^2} g\cos\theta_W \frac{g^2}{2}(V_{Hu})_{it}^*(V_{Hu})_{ic} \\
&\quad \times \big\{\big[m_{Hi}^2\big(C_0^i - C_0^j\big) + m_t^2\big(C_{11}^j + C_0^j\big)\big]\gamma^\mu P_L + \big[-2m_t C_{12}^j\big] p_c^\mu P_L\big\}.
\end{aligned}
$$

Here i, j are the color indexes and a is the index of gluon. The three-point standard functions C_0, C_{ij} are defined as

$$
\begin{aligned}
C_{ij}^a &= C_{ij}^a(-p_t, p_c, m_{Hi}, 0, m_{Hi}), \\
C_{ij}^b &= C_{ij}^b(-p_t, p_c, m_{Hi}, 0, m_{Hi}), \\
C_{ij}^c &= C_{ij}^c(-p_t, p_c, m_{Hi}, 0, m_{Hi}), \\
C_{ij}^d &= C_{ij}^d(-p_t, p_c, m_{Hi}, M_{A_H}, m_{Hi}), \\
C_{ij}^e &= C_{ij}^e(-p_t, p_c, m_{Hi}, M_{Z_H}, m_{Hi}), \\
C_{ij}^f &= C_{ij}^f(-p_t, p_c, m_{Hi}, M_{W_H}, m_{Hi}), \\
C_{ij}^g &= C_{ij}^g(-p_t, p_c, 0, m_{Hi}, 0), \\
C_{ij}^h &= C_{ij}^h(-p_t, p_c, M_{W_H}, m_{Hi}, M_{W_H}), \\
C_{ij}^i &= C_{ij}^i(-p_t, p_c, M_{W_H}, m_{Hi}, 0), \\
C_{ij}^j &= C_{ij}^j(-p_t, p_c, 0, m_{Hi}, M_{W_H}).
\end{aligned}
$$

Appendix B. The definitions of the standard functions

The definitions of the two-point and three-point standard functions have been given in Ref. [34], here we only show their definitions and explicit expressions related to our calculation.

The functions A_0, B_0, B_μ, C_0, C_μ, $C_{\mu\nu}$ are defined as

$$
\begin{aligned}
&\frac{i}{16\pi^2} A_0(m) = \mu^{2\epsilon}\int \frac{d^n q}{(2\pi)^n}\frac{1}{q^2 - m^2}, \\
&\frac{i}{16\pi^2} B_0, B_\mu(p, m_1, m_2) = \mu^{2\epsilon}\int \frac{d^n q}{(2\pi)^n}\frac{1, q_\mu}{(q^2 - m_1^2)[(q+p)^2 - m_2^2]},
\end{aligned}
$$

$$\frac{i}{16\pi^2}C_0, C_\mu, C_{\mu\nu}(p,k,m_1,m_2,m_3) = \mu^{2\epsilon}\int \frac{d^nq}{(2\pi)^n}\frac{1, q_\mu, q_{\mu\nu}}{(q^2-m_1^2)[(q+p)^2-m_2^2][(q+p+k)^2-m_3^2]}.$$

The explicit expressions of basic functions A_0, $B_n(n=0,1)$, C_0 are

$$A_0(m) = m^2\left[\Delta - \ln\frac{m^2}{\mu^2}+1\right],$$

$$B_n(p,m_1,m_2) = \left[\frac{\Delta}{n+1} - \int_0^1 dx\, x^n \ln\frac{x^2p^2 - x(p^2+m_1^2-m_2^2)+m_1^2}{\mu^2}\right](-1)^n,$$

$$C_0(p,k,m_1,m_2,m_3) = \int_0^1 dx \int_0^x dy\left[ax^2+by^2+cxy+dx+ey+f\right]^{-1},$$

with

$$a=-k^2, \qquad b=-p^2, \qquad c=-2p\,.\,k, \qquad d=-m_2^2+m_3^2+k^2,$$
$$e=-m_1^2+m_2^2+p^2+2p\,.\,k, \qquad f=-m_3^2.$$

The definition of the divergent term Δ is

$$\Delta = \frac{1}{\epsilon} - \gamma + ln4\pi, \qquad \epsilon = 2-\frac{n}{2}.$$

The functions B_μ, C_μ, $C_{\mu\nu}$ can be obtained based on the following relations

$$B_\mu(p,m_1,m_2) = p_\mu B_1(p,m_1,m_2),$$
$$C_\mu(p,k,m_1,m_2,m_3) = p_\mu C_{11} + k_\mu C_{12},$$
$$C_{\mu\nu}(p,k,m_1,m_2,m_3) = p_{1\mu}p_{1\nu}C_{21} + p_{2\mu}p_{2\nu}C_{22} + (p_{1\mu}p_{2\nu}+p_{1\nu}p_{2\mu})C_{23} + g_{\mu\nu}C_{24},$$

and the function C_{24} is

$$C_{24}(p,k,m_1,m_2,m_3) = \frac{\Delta}{4} + \frac{1}{4}\left[1-\bar{B}_0(k,m_2,m_3) + 2m_1^2C_0 + f_1C_{11} + f_2C_{12}\right],$$

with

$$f_1 = m_1^2 - m_2^2 + p^2, \qquad f_2 = m_2^2 - m_3^2 + (p+k)^2 - p^2.$$

The explicit expressions of other three-point functions C_{ij} can be found in Ref. [34].

References

[1] G. Weiglein, et al., Phys. Rep. 426 (2006) 47.
[2] G. Eilam, J.L. Hewett, A. Soni, Phys. Rev. D 44 (1991) 1473;
G. Eilam, J.L. Hewett, A. Soni, Phys. Rev. D 59 (1999) 039901(E);
B. Mele, S. Petrarca, A. Soddu, Phys. Lett. B 435 (1998) 401;
A. Cordero-Cid, et al., Phys. Rev. D 73 (2006) 094005;
G. Eilam, M. Frank, I. Turan, Phys. Rev. D 73 (2006) 053011.
[3] N. Arkani-Hamed, A.G. Cohen, H. Georgi, Phys. Lett. B 513 (2001) 232.
[4] N. Arkani-Hamed, A.G. Cohen, E. Katz, A.E. Nelson, JHEP 0207 (2002) 034.

[5] J.L. Hewett, F.J. Petriello, T.G. Rizzo, JHEP 0310 (2003) 062;
C. Csaki, J. Hubisz, G.D. Kribs, P. Meade, J. Terning, Phys. Rev. D 67 (2003) 115002.
[6] I. Low, JHEP 0410 (2004) 067;
H.C. Cheng, I. Low, JHEP 0408 (2004) 061;
J. Hubisz, P. Meade, Phys. Rev. D 71 (2005) 035016;
J. Hubisz, S.J. Lee, G. Paz, JHEP 0606 (2006) 041.
[7] J. Hubisz, P. Meade, A. Noble, M. Perelstein, JHEP 0601 (2006) 136.
[8] For rare top quark decays in the MSSM model, see C.S. Li, R.J. Oakes, J.M. Yang, Phys. Rev. D 49 (1994) 293;
G. Couture, C. Hamzaoui, H. Konig, Phys. Rev. D 52 (1995) 1713;
J.L. Lopez, D.V. Nanopoulos, R. Rangarajan, Phys. Rev. D 56 (1997) 3100;
G.M. de Divitiis, R. Petronzio, L. Silvestrini, Nucl. Phys. B 504 (1997) 45;
J.M. Yang, B.-L. Young, X. Zhang, Phys. Rev. D 58 (1998) 055001;
J.J. Liu, C.S. Li, L.L. Yang, L.G. Jin, Phys. Lett. B 599 (2004) 92;
M. Frank, I. Turan, Phys. Rev. D 74 (2006) 073014;
J.M. Yang, C.S. Li, Phys. Rev. D 49 (1994) 3412;
J. Guasch, J. Sola, Nucl. Phys. B 562 (1999) 3;
G. Eilam, et al., Phys. Lett. B 510 (2001) 227;
J.L. Diaz-Cruz, H.-J. He, C.-P. Yuan, Phys. Lett. B 179 (2002) 530;
D. Delepine, S. Khalil, Phys. Lett. B 599 (2004) 62.
[9] For rare top quark decays in the TC2 model, see X.L. Wang, et al., Phys. Rev. D 50 (1994) 5781;
C. Yue, et al., Phys. Lett. B 508 (2001) 290;
G.R. Lu, F.R. Yin, X.L. Wang, L.D. Wan, Phys. Rev. D 68 (2003) 015002;
H. Zhang, arXiv: 0712.0151 [hep-ph].
[10] For rare top quark decays in the LHT model, see H.S. Hou, hep-ph/0703067.
[11] J.J. Cao, G. Eilam, M. Frank, K. Hikasa, G.L. Liu, I. Turan, J.M. Yang, Phys. Rev. D 75 (2007) 075021.
[12] J.J. Liu, C.S. Li, L.L. Yang, L.G. Jin, Nucl. Phys. B 705 (2005) 3;
G. Eilam, M. Frank, I. Turan, Phys. Rev. D 74 (2006) 035012;
J. Guasch, W. Hollik, S. Oenaranda, J. Sola, Nucl. Phys. B (Proc. Suppl.) 157 (2006) 152;
D. Lopez-Val, J. Guasch, J. Sola, arXiv: 0710.0587 [hep-ph].
[13] J. Cao, Z. Xiong, J.M. Yang, Phys. Rev. D 67 (2003) 071701;
J. Cao, G.L. Liu, J.M. Yang, H. Zhang, Phys. Rev. D 76 (2007) 014004;
G. Liu, H. Zhang, arXiv: 0708.1553 [hep-ph].
[14] J. Cao, Z. Xiong, J.M. Yang, Nucl. Phys. B 651 (2003) 87;
C.S. Li, X. Zhang, S.H. Zhu, Phys. Rev. D 60 (1999) 077702;
Z.H. Yu, H. Pietschmann, W.G. Ma, L. Han, Y. Jiang, Eur. Phys. J. C 16 (2000) 541.
[15] Y. Jiang, M.L. Zhou, W.G. Ma, L. Han, H. Zhou, M. Han, Phys. Rev. D 57 (1994) 4343.
[16] C. Yue, Y. Dai, Q. Xu, G. Liu, Phys. Lett. B 525 (2002) 301;
C. Yue, G. Liu, Q. Xu, Phys. Lett. B 509 (2002) 294;
C. Yue, G. Lu, J. Cao, J. Li, G. Liu, Phys. Lett. B 496 (2000) 93;
J. Cao, G. Liu, J.M. Yang, Eur. Phys. J. C 41 (2005) 381.
[17] S. Bar-Shalom, J. Wudka, Phys. Rev. D 60 (1999) 094016.
[18] C.X. Yue, J. Wen, J.Y. Liu, W. Liu, arXiv: 0803.1335 [hep-ph].
[19] For examples H.J. He, C.P. Yuan, Phys. Rev. Lett. 83 (1999) 28;
G. Burdman, Phys. Rev. Lett. 83 (1999) 2888;
J. Cao, G. Liu, J.M. Yang, Phys. Rev. D 70 (2004) 114035;
F. Larios, F. Penunuri, J. Phys. G 30 (2004) 895;
X.L. Wang, Y.L. Yang, B.Z. Li, C.X. Yue, J.Y. Zhang, Phys. Rev. D 66 (2002) 075009;
X.L. Wang, B.Z. Li, Y.L. Yang, Phys. Rev. D 68 (2003) 115003;
W. Xu, X.L. Wang, Z.J. Xiao, Eur. Phys. J. C 51 (2007) 891.
[20] J. Hubisz, S.J. Lee, G. Paz, JHEP 0606 (2006) 041.
[21] M. Blanke, A.J. Buras, A. Poschenrieder, C. Tarantino, S. Uhlig, A. Weiler, JHEP 0612 (2006) 003.
[22] M. Blanke, A.J. Buras, A. Poschenrieder, S. Recksiegel, C. Tarantino, S. Uhlig, A. Weiler, JHEP 0701 (2007) 066.
[23] M. Blanke, A.J. Buras, S. Recksiegel, C. Tarantino, S. Uhlig, Phys. Lett. B 657 (2007) 81.
[24] M. Blanke, A.J. Buras, S. Recksiegel, C. Tarantino, S. Uhlig, JHEP 0706 (2007) 082.
[25] M. Blanke, A.J. Buras, B. Duling, A. Poschenrieder, C. Tarantino, JHEP 0705 (2007) 013;
S.R. Choudhury, A.S. Cornell, A. Deandrea, N. Gaur, A. Goyal, hep-ph/0612327.

[26] X.L. Wang, H.L. Jin, Y. J Zhang, Y.H. Xi, arXiv: 0803.3011 [hep-ph], 1.
[27] J. Pumplin, A. Belyaev, J. Huston, D. Stump, W.K. Tung, JHEP 0602 (2006) 032.
[28] K. Hagiwara, D. Zeppenfeld, Nucl. Phys. B 313 (1989) 560;
V. Barger, T. Han, D. Zeppenfeld, Phys. Rev. D 41 (1990) 2782.
[29] J. Hubisz, P. Meade, A. Noble, M. Perelstein, JHEP 0601 (2006) 135.
[30] Particle Data Group, W.-M. Yao, et al., J. Phys. G 33 (2006) 1.
[31] T. Han, R.D. Peccei, X. Zhang, Nucl. Phys. B 454 (1995) 527;
L. Chikovani, T. Djobava, hep-ex/0205016;
M. Beneke, et al., hep-ph/0003033;
T. Han, K. Whisnant, B.L. Young, X. Zhang, Phys. Rev. D 55 (1997) 7241.
[32] T. Stelzer, Z. Sullivan, S. Willenbrock, Phys. Rev. D 58 (1998) 094021;
T. Han, M. Hosch, K. Whisnant, B.L. Young, X. Zhang, Phys. Rev. D 58 (1998) 073008.
[33] F. del Aguila, J.A. Aguilar-Saavedra, Nucl. Phys. B 576 (2000) 56.
[34] M. Clements, et al., Phys. Rev. D 27 (1983) 570;
A. Axelrod, Nucl. Phys. B 209 (1982) 349;
G. Passarino, M. Veltman, Nucl. Phys. B 160 (1979) 151.